# Collector Series-Resistor to Stabilize a Broadband 400 GHz Common-Base Amplifier

Jerome Cheron, Senior *Member, IEEE*, Dylan F. Williams, *Fellow, IEEE*, Richard A. Chamberlin, Miguel E. Urteaga, Senior *Member, IEEE,* Kassiopeia A. Smith, Nicholas R. Jungwirth, Bryan T. Bosworth, Christian J. Long, Nathan D. Orloff, *Senior Member, IEEE*, and Ari D. Feldman.

***Abstract*— The indium phosphide (InP) 130 nm double-heterojunction bipolar transistor (DHBT) offers milliwatts of output power and high signal amplification in the lower end of the terahertz frequency band when the transistor is used in a common-base configuration. Instrumentation can directly benefit from this technology by enabling the development of novel broadband sources or synthesizers that rely on our ability to amplify the signal over enormous bandwidths. However, the design of high gain and stable amplifiers presents many obstacles and limitations as we increase the bandwidth and the carrier frequency. Here we show that adding a series resistor at the collector terminal of the common-base transistor prevents instabilities in the terahertz monolithic integrated circuit (TMIC) amplifier and increases its fractional bandwidth. Adopting this technique, we report a state-of-the-art broadband common-base amplifier that exhibits a minimum small-signal gain of 18.9 dB from 325 GHz to 477 GHz. This amplifier presents the highest fractional bandwidth and gain above 300 GHz. Our work demonstrates the feasibility of high-performance amplifiers that address the need of future terahertz electronic systems.**

***Index Terms*— Submillimeter-wave, terahertz monolithic integrated circuit (TMIC), broadband amplifier, common-base amplifier, indium phosphide (InP), double heterojunction bipolar transistor (DHBT).**

## I. Introduction

The constant growing demand in high-speed data transfer has incited the solid-state electronic foundries to scale their technologies to frequencies that offer hundreds of gigahertz of bandwidth. Wireless telecommunication industries currently develop millimeter-wave 5G communications systems operating in allocated bands between 24 GHz and 52 GHz [1] and further investigations are led in unlicensed bands up to 92 GHz. The development of recent technologies also enables new and emerging applications above 100 GHz [2] in high resolution imaging, radio astronomy, spectroscopy, atmospheric sensing, automotive radar, and communication beyond 5G. Instrumentation naturally follows frequency operation of electronics and new equipment covering ultra-wide bandwidths must be fabricated to accurately characterize circuits that operate up to 1 THz. New sources and synthesizers that implement a multitone amplitude control and phase control capabilities will allow researchers to explore the nonlinear response of active circuits in frequency bands that are currently limited by linear scattering parameters and scalar power analyses.

The TMIC amplifier plays a key role in the development of new terahertz instrumentation. Its electrical performance grandly contributes to the specification of the final product. At the circuit level, the amplifiers must provide up to a milliwatt of output power and high-signal amplification to enable a large amplitude control at the system level. Ultra-wideband

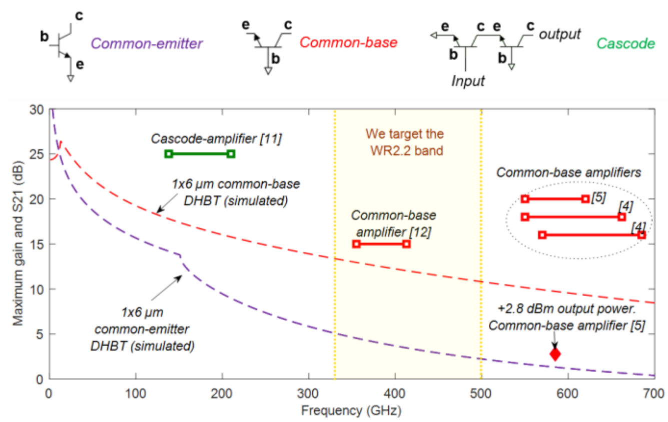


Fig. 1. Overview of the indium phosphide 130 nm double-heterojunction bipolar transistor for power amplification applications. The maximum gain of a 6 µm long emitter DHBT in a single common-emitter configuration and common-base configurations is simulated (dotted line). The minimum measured small-signal gain ($S_{21}$) of published multiple-stage amplifiers in a common-base and cascode configurations are plotted with solid lines.

Manuscript received June 18, 2021; revised September 9, 2021; accepted September 29, 2021. This work was supported by the U.S. Government. This paper is an official contribution of NIST. Usage of commercial products herein is for information only; it does not imply recommendation or endorsement by NIST. *(Corresponding author: Jerome Cheron.)*

Jerome Cheron is with the National Institute of Standards and Technology, Boulder, CO 80305 USA, and also with the Department of Physics, University of Colorado, Boulder, CO 80302 USA (e-mail: jerome.cheron@nist.gov).

Dylan F.Williams, Richard A. Chamberlin, Kassiopeia A. Smith, Nicholas R. Jungwirth, Bryan T. Bosworth, Christian J. Long, Nathan D. Orloff, and Ari D. Feldman are with the National Institute of Standards and Technology, Boulder, CO 80305 USA (e-mail: dylan.williams@nist.gov; richard.chamberlin@nist.gov; kassiopeia.smith@nist.gov; nicholas.jungwirth@nist.gov; bryan.bosworth@nist.gov; christian.long@nist.gov; nathan.orloff@nist.gov; ari.feldman@nist.gov).

Miguel E. Urteaga is with the Teledyne Scientific Company, Thousand Oaks, CA 91360 USA (e-mail: miguel.urteaga@teledyne.com).

Color versions of one or more figures in this article are available at https://doi.org/10.1109/TTHZ.2021.3119999.

Digital Object Identifier 10.1109/TTHZ.2021.3119999.

amplifiers will also facilitate the circuits integration and relax the system complexity.

Several TMIC amplifiers based on III-V semiconductors, operating in the 0.3 THz – 1 THz frequency band, have been reported over the past decades. These circuits have been designed to demonstrate the feasibility of new applications above 300 GHz. Amplifiers fabricated on a 25 nm indium phosphide high-electron-mobility transistor (HEMT) have demonstrated amplification at 1 THz [3] when the InP 130 nm DHBT process has exhibited high-gain performance up to 670 GHz [4] and delivered over a milliwatt of output power at 585 GHz [5]. Recently, a broadband amplifier fabricated on a 35 nm indium gallium arsenide (InGaAs) metamorphic high-electron-mobility transistor (mHEMT) process has covered 150 GHz of bandwidth at a central frequency of 355 GHz [6].

In this study, we use the InP 130 nm DHBT process [7] to design a broadband, single-ended amplifier in a common-base configuration within the WR2.2 waveguide band. Although several common-base amplifiers in diverse InP DHBT processes have been demonstrated above 100 GHz [4, 5, 8, 9], stability is always a critical step of the amplifier design. In the following paragraphs, we first present the technological properties before depicting design methodology with a specific focus on the proposed stability technique that we adopted on the common-base transistor. Finally, we measure the amplifier and compare the performance with other TMIC amplifiers published in the literature.

## II. 130 nm InP DHBT TMIC Technology

Integrated circuits in the InP 130 nm DHBT process have demonstrated diverse functionalities above 300 GHz [10]. A 2 µm long emitter DHBT exhibits a current gain cutoff frequency $f_t$ = 520 GHz and a maximum frequency of oscillation $f_{max}$ = 1.1 THz. The DHBTs have a common-emitter breakdown voltage of 3.5 V and a maximum current emitter density $J_E$ = 25 mA/µm$^2$ at $V_{CE}$=2.0 V. Fig. 1 illustrates the capability of this technology to amplify signal up to 700 GHz. The common-base configuration presents a smaller Miller capacitance than the common-emitter configuration, and consequently exhibits a higher maximum available/stable gain at high frequencies. The cascode configuration will provide performance that varies between the maximum gain of a common-base configuration and a common-emitter configuration. The physical connection designed between the collector of the first transistor and the emitter of the second transistor directly impacts the maximum gain response of the cascode topology. At an equivalent bias point, $J_E$ = 20 mA/µm$^2$ at $V_{CE}$=1.9 V (or $V_{CB}$=1.0 V), a 6 µm long emitter in a common-base configuration exhibits a maximum available gain higher than 9 dB up to 700 GHz, while the common-emitter provides at least 9 dB of maximum available/stable gain up to 210 GHz only. The common-emitter and cascode configuration will be preferred at lower frequencies since the conditions of stability are easier to achieve. As shown in Fig. 1, the common-emitter configuration is being unconditionally stable above 160 GHz (K point). Recently, a cascode amplifier has provided over 25 dB of small-signal gain up to 200 GHz [11]. The common-base topology will be used to target the highest frequencies. Amplifiers have already been demonstrated above 500 GHz [4, 5]. In this work, we will use 6 µm long emitter DHBTs to design a broadband, single-ended common-base amplifier around 400 GHz.

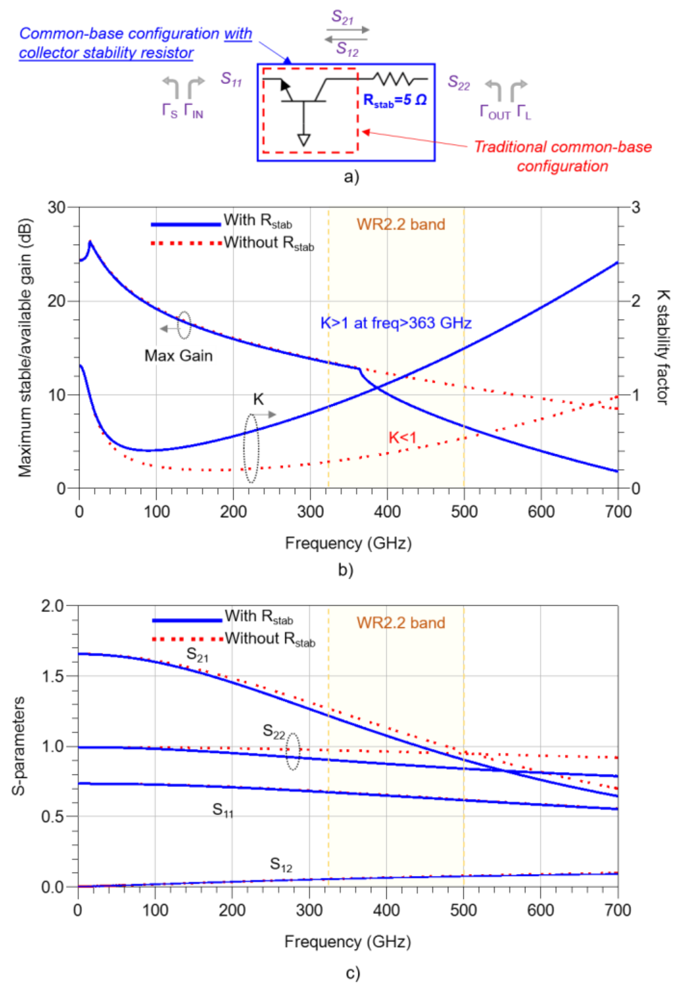


Fig. 2. Linear stability analysis for (a) two configurations of an InP 130 nm 6 µm long emitter common-base DHBT with and without a 5-ohm series resistor at the collector terminal. (b) simulations of the maximum available/stable gain and K stability factor and, (c) the S-parameters. The bias points are set at $V_{CB}$=1.0 V and $J_E$= 20 mA/µm$^2$.

## III. Broadband Power-Amplifier Design

### A. Linear stability of a 6 µm long emitter common-base DHBT

The stability condition of transistor in a common-base configuration may dramatically change with the variation of parasitic elements in the design, such an extra inductance connecting the base of the transistor with the ground plane, a coupling effects between the collector and the emitter, or an undesired positive feedback. Some design techniques have been explored to improve stability conditions. For instance, the differential common-base topology [5, 12] reduces the risk of oscillations caused by the parasitic inductance of the passive elements that connects the base of the transistor to the ground plane. However, the overall design implementation is more complex since it requires a (0/180)° power divider and combiner. A negative feedback technique has been successfully demonstrated on differential common-base amplifiers [5] but this approach is more difficult to implement on single-ended topology, whereas resistive feedback [9] has been preferred.

In this study, we propose a solution that consists of adding a series resistor at the output of the transistor, at the collector terminal. This method, mentioned in [13], has not been practically demonstrated on any topologies of high-frequency integrated amplifiers. Circuit-designers tend to preserve the delivered output-power and consequently avoid using any resistive element on the output matching network. Traditionally, circuit-designers would place a series resistor at the input terminal of the transistor to improve the in-band stability, but this technique is not effective with an InP 130 nm DHBT in a common-base configuration, the input reflection coefficient of the device being relatively low. The input series-resistor is usually very effective with common-source and common-emitter transistors that present a high input reflection coefficient. In this case, the series resistor reduces the gain and favorably pre-matches the input impedance of the transistor.

Designing amplifiers in a common-base configuration requires a specific attention to the conventional stability analyses, such the K factor [14], the source and load stability circles [13], and the loop gain as the Normalized Determinant Function (NDF) [15] while many transistors are used in parallel and multiple amplification stages are designed.

Practically, instabilities occur if any passive source and load terminations of the transistor, $Z_S$ and $Z_L$, respectively, generate output or input impedances, $Z_{OUT}$ and $Z_{IN}$, having a real negative part. In term of reflection coefficients, the conditions for unconditional stability are given by:

$$|\Gamma_{IN}| = \left|S_{11} + \frac{S_{12}S_{21}\Gamma_L}{1-S_{22}\Gamma_L}\right| < 1 \quad (1)$$

$$|\Gamma_{OUT}| = \left|S_{22} + \frac{S_{12}S_{21}\Gamma_S}{1-S_{11}\Gamma_S}\right| < 1 \quad (2)$$

To demonstrate the feasibility of the proposed method, we study the linear stability for the common-base configuration with and without an ideal 5 ohms series resistor on the collector, as illustrated in Fig. 2(a). We use the foundry's nonlinear ADS[1]-HBT model to perform the simulations and design the amplifier. The transistor is biased at the emitter current density $J_E$ = 20 mA/μm$^2$ and $V_{CB}$ = 1.0 V. For both configurations, we simulate and plot the K stability factor and the maximum gain in Fig. 2(b), and the S-parameters in Fig. 2(c). A transistor is considered unconditionally stable if K > 1, with delta (Δ) < 1 [13, 14]. Looking first at the configuration without resistor (dotted line), the K factor indicates that the device is potentially unstable over the frequency band (K < 1). Identifying the S-parameters with the equations (1) and (2) provides insights on the overall stability conditions. The $S_{21}$ being very low and the $S_{22}$ very high, i.e. $|S_{22}| \approx 1$, and assuming an optimal small-signal gain impedance matching, i.e. $\Gamma_S \approx S^*_{11}$ and $\Gamma_L \approx S^*_{22}$, we identify $S_{22}$ as the critical parameter that considerably deteriorates the condition of stability. Its high magnitude may cause $|\Gamma_{OUT}| > 1$ and $|\Gamma_{IN}| > 1$ and so decreasing $S_{22}$ will consequently relax the overall stability conditions. It can be achieved by adding a small resistive element in series at the collector terminal. This solution is valuable only if the

[1]We identify commercial products only to accurately describe the experiments and analysis we performed. NIST does not endorse commercial products. Other products may work as well or better.

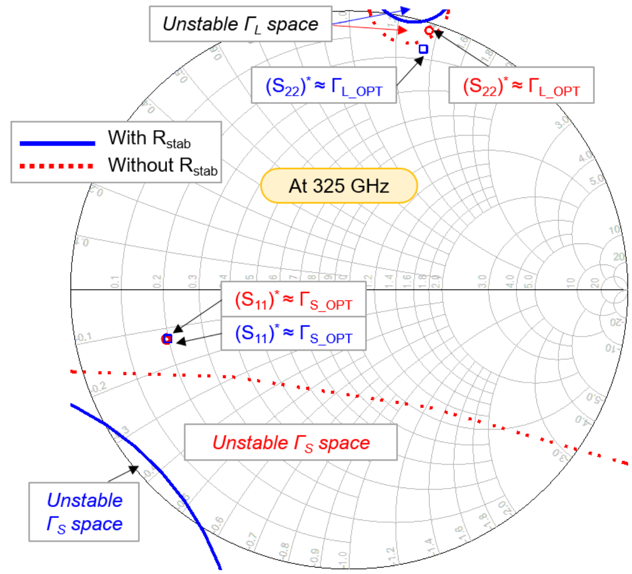


Fig. 3. Source and load stability circles simulated for a 6 μm long emitter common-base DHBT at 325 GHz without resistor (red - dotted lines), and with a series resistor at the collector terminal (blue - solid line). $V_{CB}$=1.0 V and $J_E$= 20 mA/μm$^2$.

maximum available gain is significantly high, so the transistor still provides a satisfying maximum stable gain when terminated with a 5-ohm series resistor. In the targeted frequency band, the common-base configuration, without resistor, exhibits a maximum available gain higher than 11 dB up to 500 GHz.

The addition of a 5-ohm series resistor at the collector terminal, creating a low-pass filter with the output capacitance of the transistor, slightly decreases the $S_{22}$ around a value of 0.9 at the highest frequencies, but it considerably improves the stability conditions. The analyses of the K stability factor and the maximum gain clearly highlight the benefit of the 5-ohm series resistor. This configuration is unconditionally stable above 363 GHz, with a maximum stable gain higher than 6 dB from 363 GHz to 500 GHz. Below 363 GHz, the device remains potentially unstable. Increasing the series resistor value will dramatically decrease the maximum stable gain in the upper band, making amplification impossible. In the lower band, from 325 GHz to 363 GHz, we must choose a stable set of source and load impedances, accordingly to the stability circles. To determine the source and load terminations, $\Gamma_S$ and $\Gamma_L$, that produce a negative impedance at a given frequency, we plot the circles for $|\Gamma_{OUT}|$=1 and $|\Gamma_{IN}|$=1, defining the boundaries between the stable and unstable spaces on the smith chart [13]. Fig. 3 illustrates the unstable source and load spaces at 325 GHz, for the two proposed configurations. We also plot the $\Gamma_{S\_OPT} \approx S^*_{11}$ and $\Gamma_{L\_OPT} \approx S^*_{22}$, which correspond to the optimal source and load impedances that provide high small-signal gain.

Looking at the configuration without a resistor, we observe two aspects that clearly increase the chance of oscillations: 1) the space of source impedances producing $|\Gamma_{OUT}| > 1$ is significantly large and, 2) the optimal targeted source impedance, $\Gamma_{S\_OPT}$, is located near the circle boundary. Designing under these conditions is critical since any small design imperfections, perturbations, process variation or any minor transistor model imprecisions may dramatically increase the unstable impedance space and consequently changes the

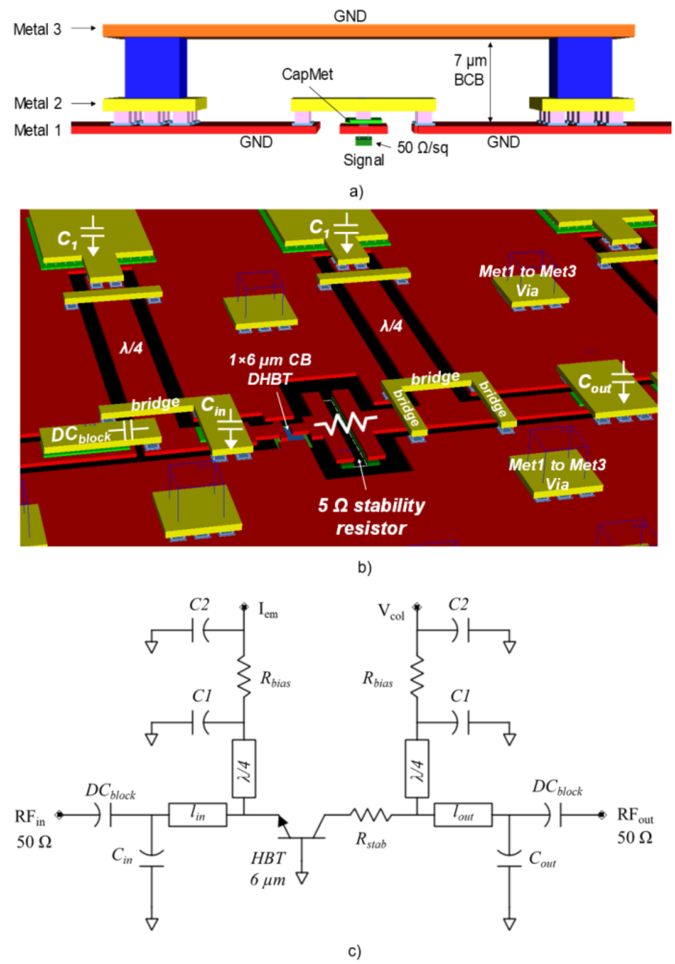


Fig. 4. (a) Cross section of the InP 130 nm passive-circuit process, (b) illustration of a 1-stage amplifier block, metal 3 is disabled, and (c) circuit schematic of the 1-stage amplifier block.

stability conditions. Alternately, the addition of the 5-ohm series resistor at the collector terminal almost clears the smith chart of unstable source impedances and provides a safer space of design around $\Gamma_{S\_OPT}$. Although the K factor indicates that this configuration remains potentially unstable below 363 GHz, we consider that the new source space of design is large enough to safely match the input impedance. Regarding the load stability circle, the impact of the collector resistor on the load impedances producing $|\Gamma_{IN}| > 1$ is not notable, even if the new $\Gamma_{L\_OPT}$ presents a lower magnitude, which will favor the broadband operation. In practice, we will match the output transistor at a $\Gamma_L$ below 0.7 which represents a good tradeoff between gain, delivered output power, stability and insertion loss in the output matching network.

### *B. Circuit Design*

The passive integrated-circuit process is illustrated in Fig. 4(a). It uses a 3-level interconnect embedded into a 7 µm thick benzo-cyclobutene (BCB) layer. This process allows us to design circuits with coplanar waveguide grounded (CPW-G) lines, where the conductor and the ground can be directly connected to the transistor terminals with Met1. This direct connection grandly facilitates the design of the matching networks and reduces the equivalent inductance that connects the base of the transistor to the ground plane. The top metal

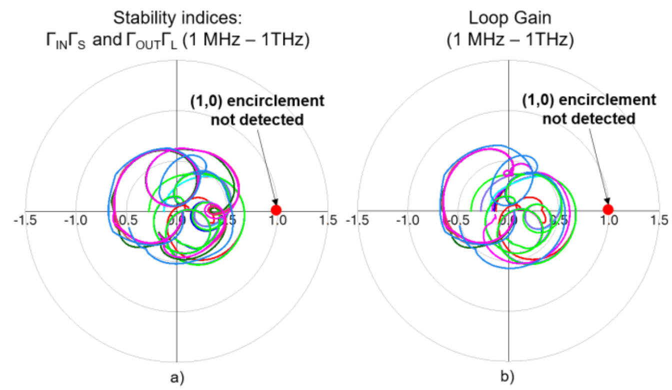


Fig. 5. Simulation of the stability indices (a) and the loop gain (b) of the 6-stage common-base amplifier. $V_{CB}$=1.0 V and $J_E$= 20 mA/µm$^2$.

layer (metal 3) is also connected to the ground of metal 1, except for DC and RF pad accesses. The integrated circuit process also includes a 0.3 fF/µm$^2$ metal-insulator-metal (MIM) capacitor layer and a 50 Ω/sq thin-film resistor layer.

We first design a 1-stage power amplifier adopting the 5-ohm series resistor configuration at the collector terminal, and match the input and output on 50 ohms. We optimize the matching networks with the objective to minimize the insertion loss and to match the optimal source and load impedances at the highest frequencies, where the gain is limited. The input and output matching networks have an insertion loss of only 1.2 dB at 475 GHz, and 2.2 dB at 325 GHz. As a result, we obtain an ideal gain of 6.8 dB at 325 GHz and 4 dB at 475 GHz for a one-stage amplifier. The impedance mismatch being more important in the lower frequency band, a maximum gain of 5.5 dB is expected below 400 GHz.

Practically, a series resistor of 3 to 4 ohms would have satisfied the stability conditions within the targeted band. However, designing resistors smaller than 5 ohms with the available 50 Ω/sq thin-film resistor layer will generate important design constraints. The matching networks and the circuit schematic of the one-stage amplifier block is illustrated in Fig. 4(b) and Fig. 4(c) respectively. We use MIM capacitors and CPW-G lines to design the RF input and output matching networks. All circuit elements are simulated using the ADS[1] momentum software. It is extremely important to simulate the physical layout of the designed resistor since this element in not purely resistive.

Fabrication tolerance must be considered during the design process. Although the value regarding the resistor layer is reliable, extra caution is required when designing the MIM capacitors $DC_{block}$, $C_{in}$ and $C_{out}$ since we use values as low as 8 fF. We perform a sensitivity analysis on the SiN layer forming the MIM capacitor by applying ± 10 % on the thickness, and we check that the simulated performance is still acceptable within this range. The tolerances are provided by the foundry. We also verify that the one-stage amplifier block does not provide any gain at microwave frequencies, avoiding potential out-of-band oscillations.

The addition of the 5-ohm series resistor naturally generates insertion loss in the circuits and modifies the linear and nonlinear responses of the transistor. From 325 GHz to 500

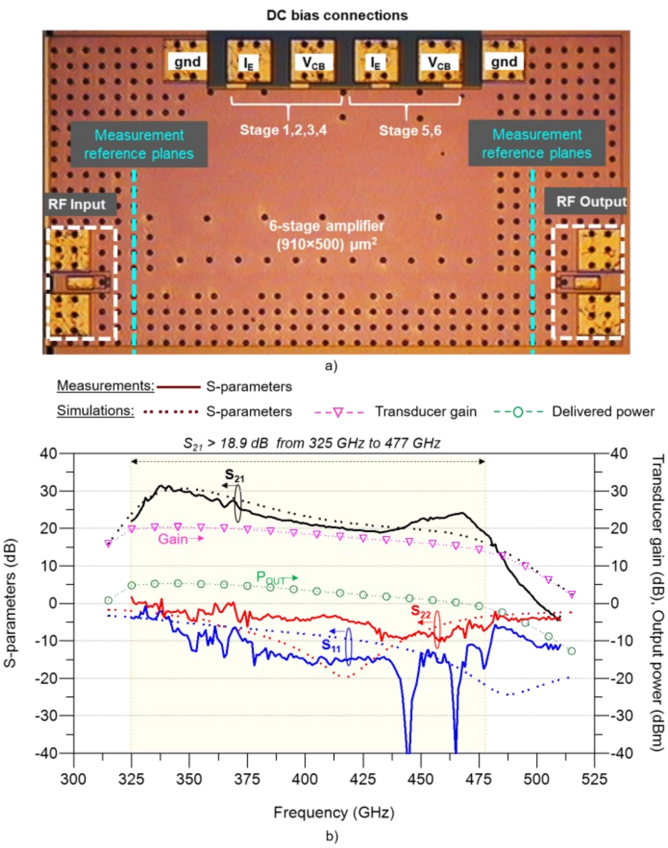


Fig. 6 (a) Photograph of the fabricated six-stage TMIC amplifier and (b) comparison between measured (solid line) and simulated (dashed line) S-parameters results of the 6-stage common-base amplifier. The transducer power gain and delivered output power are simulated near the saturation, for an available input power of -15 dBm. $V_{CB}$=0.81 V and $J_E$= 20 mA/µm$^2$.

GHz, we have seen that the new common-base configuration still provides a satisfying maximum gain, as illustrated in Fig. 2(b). However, the insertion of the 5-ohm series resistor limits the saturated output power. We perform load-pull simulations on the two common-base configurations to evaluate the impact on the series resistor near the saturation. We choose the optimal loads that provide the maximum output power at 325 GHz and 500 GHz, for 3 dB and 2 dB of power gain, respectively. The common-base configuration without resistor provides up to 9.6 dBm of output power at 325 GHz and 6.9 dBm at 500 GHz while the configuration with the 5-ohm series resistor achieves up to 8.3 dBm of output power at 325 GHz and 5.4 dBm at 500 GHz. On the overall frequency band, we estimate that the series resistor reduces the output power by 1.3 dB to 1.5 dB near the saturation. However, the addition of the series resistor favorably pre-matches the output of the transistor. The optimal loads ($\Gamma_{L\_OPT}$) are obtained at a lower magnitude, 0.1 in average, over the WR2.2 frequency band. This will facilitate the broadband matching network and will slightly reduce the insertion loss of the output matching network.

The final amplifier is realized by cascading six single-stage blocks. We perform a stability analysis based on the S-probe [16] and loop gain [17] techniques at each transistor terminal. We simulated and verified that the product of the reflection coefficients, in Fig. 5(a), and the loop gain, in Fig. 5(b), do not provide any encirclement of the polar point (1,0). We perform

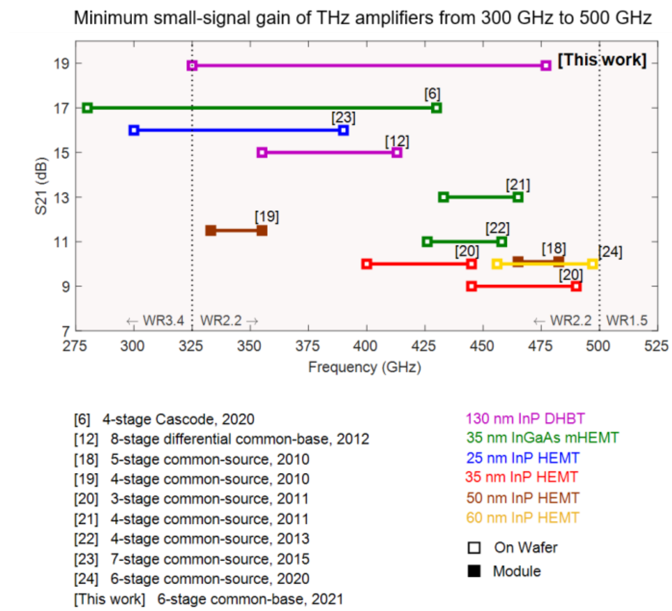


Fig. 7 State-of-the-art amplifiers in III-V semiconductor-based technologies. Minimum small-signal gain versus bandwidth from 300 GHz to 500 GHz.

the analysis form 1 MHz to 1 THz. This study corresponds to the last step of the design process.

## IV. Measurement Results

A photograph of the fabricated six-stage TMIC power amplifier is shown in Fig. 6(a). We used a Keysight PNA-X[1] and WR2.2 OML[1] extender heads to measure the S-parameters. We performed the measurement on-wafer and applied a multi-line thru-reflect-line (TRL) calibration to define the measurement reference planes directly on the lines of the ciruit, as indicated in the Fig. 6(a). A comparison between the measurement results and the simulated performance is plotted in Fig. 6(b). The measured small-signal gain exceeds 18.9 dB from 325 GHz to 477 GHz with a peak of 31 dB at 341 GHz. We observe a good agreement between measurements and simulations, even if the measured $S_{22}$ is mismatched in the upper band. Nevertheless, this TMIC amplifier demonstrates state-of-the-art performance in terms of small-signal gain over wide bandwidth. We also simulated the power gain and the delivered output power as an indication of the performance we expect near the saturation.

The measured performance has been obtained after a single circuit iteration. Our primary intention was to demonstrate the effectiveness of the series resistor on the collector of a common-base configuration. This technique improves the amplifier stability in addition of achieving wideband performance around 400 GHz. This proposed design architecture could easily be scaled to extend the bandwidth up to 500 GHz and to entirely cover the WR2.2 waveguide band. In the Fig. 7, we compare the minimum small-signal gain provided by the six-stage, single-ended common-base amplifier with other circuits published in the literature. Some of the amplifiers referenced in this graph may not have been designed for wideband applications. The performance displayed in terms of minimum small-signal gain versus bandwidth may not reflect their primary performance. To the best of the authors' knowledge, this is also the first time that the stability of a TMIC common-base amplifier is achieved with a series resistor at the collector terminal.

## V. Conclusion

We demonstrated a TMIC amplifier exhibiting a minimum small-signal gain of 18.9 dB over 152 GHz of bandwidth at a central frequency of 401 GHz. This performance, corresponding to the widest fractional bandwidth (37.9%) reported above 300 GHz, satisfies the needs of novel instrumentation. The addition of a series resistor at the collector terminal leads to several advantages when designing with a common-base configuration: (1) it ensures high and stable gain amplification, (2) it increases the amplifier bandwidth and (3), this robust design technique, including the presented stability technique and the sensitivity analysis of the MIM capacitor layer, improves the chance of obtaining the desired performance after a single circuit fabrication. This last aspect is significant for industries and research laboratories designing TMIC amplifiers since it considerably reduces the cost and the production time associated with two fabrications.

## Acknowledgment

The authors would like to thank Dr. Zach Griffith, from Teledyne Scientific, and Dr. Erich Grossman, from the National Institute of Standards and Technology (NIST) for their critical reviews.

## References

[1] 3rd Generation Partnership Project; Technical Specification Group Radio Access Network; NR; User Equipment (UE) radio transmission and reception; Part 1: Range 1 Standalone (Release 15), 3GPP TS 38.101-1 V15.12.0 (2021-01).

[2] T. S. Rappaport et al., "Wireless Communications and Applications Above 100 GHz: Opportunities and Challenges for 6G and Beyond," in IEEE Access, vol. 7, pp. 78729-78757, 2019, doi: 10.1109/ACCESS.2019.2921522.

[3] X. Mei et al., "First Demonstration of Amplification at 1 THz Using 25-nm InP High Electron Mobility Transistor Process," in IEEE Electron Device Letters, vol. 36, no. 4, pp. 327-329, April 2015, doi: 10.1109/LED.2015.2407193.

[4] J. Hacker, M. Urteaga, M. Seo, A. Skalare and R. Lin, "InP HBT amplifier MMICs operating to 0.67 THz," 2013 IEEE MTT-S International Microwave Symposium Digest (MTT), Seattle, WA, USA, 2013, pp. 1-3, doi: 10.1109/MWSYM.2013.6697518.

[5] M. Seo et al., "A 600 GHz InP HBT amplifier using cross-coupled feedback stabilization and dual-Differential Power Combining," 2013 IEEE MTT-S International Microwave Symposium Digest (MTT), Seattle, WA, USA, 2013, pp. 1-3, doi: 10.1109/MWSYM.2013.6697692.

[6] B. Gashi et al., "Broadband and High-Gain 400-GHz InGaAs mHEMT Medium-Power Amplifier S-MMIC," 2020 IEEE/MTT-S International Microwave Symposium (IMS), Los Angeles, CA, USA, 2020, pp. 484-487, doi: 10.1109/IMS30576.2020.9223968.

[7] M. Urteaga, R. Pierson, P. Rowell, V. Jain, E. Lobisser and M. J. W. Rodwell, "130nm InP DHBTs with ft >0.52THz and fmax >1.1THz," 69th Device Research Conference, Santa Barbara, CA, USA, 2011, pp. 281-282, doi: 10.1109/DRC.2011.5994532.

[8] J. Cheron and E. Grossman, "High gain 220GHz power amplifier MMICs with minimal footprint," 2016 IEEE MTT-S International Microwave Symposium (IMS), San Francisco, CA, USA, 2016, pp. 1-3, doi: 10.1109/MWSYM.2016.7540038.

[9] K. Eriksson, V. Vassilev and H. Zirath, "H-band MMIC amplifiers in 250 nm InP DHBT," 2012 19th International Conference on Microwaves, Radar & Wireless Communications, Warsaw, Poland, 2012, pp. 744-747, doi: 10.1109/MIKON.2012.6233636.

[10] M. Urteaga, Z. Griffith, M. Seo, J. Hacker and M. J. W. Rodwell, "InP HBT Technologies for THz Integrated Circuits," in Proceedings of the IEEE, vol. 105, no. 6, pp. 1051-1067, June 2017, doi: 10.1109/JPROC.2017.2692178.

[11] M. Bao, V. Vassilev, D. Gustafsson and H. Zirath, "G-band Power Amplifiers in 130 nm InP Technology," 2020 15th European Microwave Integrated Circuits Conference (EuMIC), Utrecht, Netherlands, 2021, pp. 5-8, doi: 10.1109/EuMIC48047.2021.00013.

[12] J. Hacker et al., "400 GHz HBT Differential Amplifier Using Unbalanced Feed Networks," in IEEE Microwave and Wireless Components Letters, vol. 22, no. 10, pp. 536-538, Oct. 2012, doi: 10.1109/LMWC.2012.2214767.

[13] J. Rollett, "Stability and Power-Gain Invariants of Linear Twoports," in IRE Transactions on Circuit Theory, vol. 9, no. 1, pp. 29-32, March 1962, doi: 10.1109/TCT.1962.1086854.

[14] G. Gonzalez, "Microwave Transistor Amplifier Desing," in Microwave Transistor Amplifiers: Analysis and Design, 2nd ed., Upper Saddle River, NJ: Prentice-Hall, 1997, pp. 217–272.

[15] W. Struble and A. Platzker, "A rigorous yet simple method for determining stability of linear N-port networks [and MMIC application]," 15th Annual GaAs IC Symposium, San Jose, CA, USA, 1993, pp. 251-254, doi: 10.1109/GAAS.1993.394458.

[16] K. Wang, M. Jones and S. Nelson, "The S-probe-a new, cost-effective, 4-gamma method for evaluating multi-stage amplifier stability," 1992 IEEE MTT-S Microwave Symposium Digest, Albuquerque, NM, USA, 1992, pp. 829-832 vol.2, doi: 10.1109/MWSYM.1992.188116.

[17] M. Ohtomo, "Stability analysis and numerical simulation of multidevice amplifiers," in IEEE Transactions on Microwave Theory and Techniques, vol. 41, no. 6, pp. 983-991, June-July 1993, doi: 10.1109/22.238513.

[18] V. Radisic et al., "A 10-mW Submillimeter-Wave Solid-State Power-Amplifier Module," in IEEE Transactions on Microwave Theory and Techniques, vol. 58, no. 7, pp. 1903-1909, July 2010, doi: 10.1109/TMTT.2010.2050105.

[19] W. R. Deal et al., "Demonstration of a 0.48 THz Amplifier Module Using InP HEMT Transistors," in IEEE Microwave and Wireless Components Letters, vol. 20, no. 5, pp. 289-291, May 2010, doi: 10.1109/LMWC.2010.2045597.

[20] L. Samoska et al., "On-wafer measurements of S-MMIC amplifiers from 400–500 GHz," 2011 IEEE MTT-S International Microwave Symposium, Baltimore, MD, USA, 2011, pp. 1-4, doi: 10.1109/MWSYM.2011.5972616.

[21] A. Tessmann et al., "Metamorphic HEMT MMICs and Modules Operating Between 300 and 500 GHz," in IEEE Journal of Solid-State Circuits, vol. 46, no. 10, pp. 2193-2202, Oct. 2011, doi: 10.1109/JSSC.2011.2163212.

[22] U. J. Lewark et al., "A 440 GHz balanced active frequency multiplier-by-four SMMIC," 2013 European Microwave Integrated Circuit Conference, Nuremberg, Germany, 2013, pp. 216-219.

[23] A. Zamora et al., "A Submillimeter Wave InP HEMT Multiplier Chain," in IEEE Microwave and Wireless Components Letters, vol. 25, no. 9, pp. 591-593, Sept. 2015, doi: 10.1109/LMWC.2015.2451364.

[24] H. Hamada, T. Tsutsumi, H. Matsuzaki, H. Sugiyama and H. Nosaka, "475-GHz 20-dB-Gain InP-HEMT Power Amplifier Using Neutralized Common-Source Architecture," 2020 IEEE/MTT-S International Microwave Symposium (IMS), Los Angeles, CA, USA, 2020, pp. 1121-1124, doi: 10.1109/IMS30576.2020.9223851.

**Jerome Cheron** (Senior Member, IEEE) received the Ph.D. degree in electrical engineering from the University of Limoges, France, in 2011. He was involved in a research project with the XLIM Laboratory, Limoges, and Thales LAS France, Rungis, France. He developed a packaging methodology of GaN HEMTs

dedicated to the design of high efficiency and wideband amplifiers for radar applications at S-Band frequencies.
In 2012, he was a PostDoctoral Fellow with Fraunhofer Institute for Applied Solid State Physics, Freiburg, Germany, where he designed high-efficiency GaN power amplifiers at Ka-band frequencies.
In 2013, he joined the National Institute of Standards and Technology, Boulder, CO, USA. His current research interests include the modeling and design of millimeter-wave and terahertz active-circuits in III-V technologies.

**Dylan F. Williams** (Fellow, IEEE) received the Ph.D. degree in electrical engineering from the University of California at Berkeley, Berkeley, CA, USA, in 1986.
He joined the Electromagnetic Fields Division, National Institute of Standards and Technology, Boulder, CO, USA, in 1989, where he currently develops electrical waveform and microwave metrology. He has authored or coauthored over 100 technical articles.
Dr. Williams was a recipient of the Department of Commerce Bronze and Silver Medals, the Astin Measurement Science Award, the Electrical Engineering Laboratory's Outstanding Paper Award two times, the Automatic RF Techniques Group (ARFTG) Best Paper Award three times, the ARFTG Automated Measurements Technology Award, the IEEE Morris E. Leeds Award, the European Microwave Prize, and the 2013 IEEE Joseph F. Keithley Award. He has served as the 2017 President of the IEEE Microwave Theory and Techniques Society. He also served as an Editor for the IEEE TRANSACTIONS ON MICROWAVE THEORY AND TECHNIQUES from 2006 to 2010 and the Executive Editor of the IEEE TRANSACTIONS ON TERAHERTZ SCIENCE AND TECHNOLOGY.

**Richard A. Chamberlin**, National Institute of Standards and Technology (NIST) Boulder, was graduated from the University of California (Santa Barbara, CA) with a B.S. in physics in 1984, and obtained his Ph.D. in physics from the Massachusetts Institute of Technology (Cambridge, MA) in 1991. He served in the United States Air Force from 1975 to 1979 as a Weather Observer. In 1995 he was the first winter-over scientist with the pioneering Antarctic Submillimeter Telescope and Remote Observatory which he helped design, build, and test while at Boston University. From 1996 to 2010 he was the Technical Manager of the Caltech Submillimeter Observatory located on the summit of Mauna Kea on the Island of Hawaii. Currently he is with the High-Speed Electronics Group at NIST where he contributes to projects at millimeter-wave and terahertz frequencies and is developing a fully automated microwave wafer probing system for millikelvin temperatures.

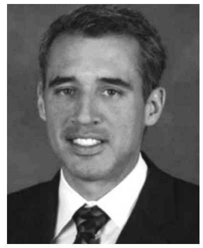

**Miguel E. Urteaga** (Senior Member, IEEE) received the M.S. and Ph.D. degrees in electrical engineering from the University of California Santa Barbara, Santa Barbara, CA, USA, in 2001 and 2003, respectively. He is the Manager of Teledyne Scientific Company's advanced device development group. His research is focused on the development of ultrahigh-speed transistor technologies, primarily in the InP material system. He has led the development of Teledyne's high-performance InP HBT IC technologies. These technologies have been used to demonstrate state-of-the-art integrated circuits ranging from high-speed mixed-signal and digital ICs to mm-wave and THz monolithic integrated circuits. He served as the program manager at Teledyne for the DARPA THz Electronics and Diverse Accessible Heterogeneous Integration (DAHI) programs. He has authored or coauthored over 100 conference and journal publications.

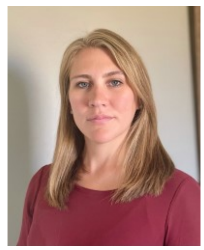

**Kassiopeia A. Smith** Kassiopeia Smith received a Ph.D. degree in materials science and engineering from Boise State University in Boise, Idaho in 2018. In 2018, she was a Post-Doctoral Fellow with the National Institute of Standards and Technologies in Boulder, Colorado. In 2021, she joined 5th Gait Technologies as a Senior Scientist in Colorado Springs, Colorado. Her current research interests include electronic and opto-electronic survivability testing in extreme environments.

**Nicholas R. Jungwirth** was born in Phoenix, Arizona in 1988. He earned B.S. degrees in physics and mathematics from Barrett, The Honors College at Arizona State University in 2011 and the PhD degree in Physics from Cornell University in Ithaca, New York in 2018. His doctoral thesis focused on discovering new defect-based single photon sources in wide bandgap semiconductors including zinc oxide and hexagonal boron nitride.
In 2018, he began his postdoctoral research at the University of Colorado Boulder and the National Institute of Standards and Technology (NIST). He is currently a National Research Council (NRC) Fellow at NIST Boulder.

**Bryan T. Bosworth** received the B.S.E degree in electrical engineering from Princeton University in 2009. He was a Fulbright scholar at the University of Freiburg until 2011 and then received the Ph.D. degree in electrical and computer engineering from Johns Hopkins University in 2017.
He joined the National Institute of Standards and Technology (NIST) in Boulder, CO as a postdoctoral researcher in 2018. In 2019, he was awarded a National Research Council Fellowship. His research focuses on optoelectronic high frequency waveform synthesis and measurement.

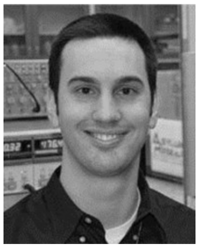

**Christian J. Long** received the B.S. and Ph.D. degrees in physics from the University of Maryland at College Park, College Park, MD, USA, in 2004 and 2011, respectively. His doctoral research focused on the development of both microwave near-field scanning probe microscopy techniques and new methods to analyze data from combinatorial materials experiments. From 2012 to 2015, he was a Post-Doctoral Researcher with the National Institute of Standards and Technology (NIST), Gaithersburg, MD, where he focused on techniques for characterizing nanoscale materials. In 2016, he joined NIST, Boulder, CO, USA, as a staff, where he currently leads a project on the development of on-chip standards for microwave and millimeter-wave calibration.

**Nathan D. Orloff** (Senior Member, IEEE) received the B.S. degree in physics with high honors and Ph.D. degree in physics from the University of Maryland (UMD) at College Park, College Park, MD, USA, in 2004 and 2010, respectively. His doctoral thesis concerned the study and measurement of microwave properties of Ruddelsden-Popper ferroelectrics. In 2014, he joined the Communications Technology Laboratory at NIST in Boulder Colorado. Dr. Orloff is currently the Project Leader of the Microwave Materials Project in the Communications Technology Laboratory at NIST in Boulder, Colorado. His research covers materials-by-design for communications, microwave materials metrology, and bridging the gap between optical and microwave on-wafer measurement science. Dr. Orloff received the 2020 Department of Commerce Bronze Medal and the 2019 American Ceramic Society Karl Schwartzwalder-Professional Achievement in Ceramic Engineering (PACE) Award for contributions to dielectric measurement. He has published over 60 publications and conference proceedings.

**Ari D. Feldman** received his B.S. in Engineering Physics in 2006 and Ph.D. in Materials Science in 2012 from the Colorado school of Mines, Golden, CO, USA. His doctoral thesis involved the study of anomalous photoconductive decay behavior in silicon under high-optical-injection conditions. Continuing his research on photodetectors, in 2012 he joined the Sensors and Detectors Group as a post-doctoral researcher at the National Institute of Standards and Technology, Boulder, CO. In the Fall of 2013, he was awarded the National Research Council Post-Doctoral Fellowship and joined the High-Speed Measurements Group to develop high-speed photodetectors. As a staff researcher he has contributed to a variety of projects including the Department of Commerce Gold Award winning LTE Impacts on GPS. As of the spring of 2019, he is the Group Leader for the High-Speed Measurements Group and Project Leader for the Waveform Metrology Project. Research interests include on-wafer metrology, electro-optic sampling, high-speed photodetectors, and integrated photonics.